Optimized interpretation of fractional flow reserve derived from computed tomography: Comparison of three interpretation methods

著者	Hidenobu Takagi, Yu Ishikawa, Makoto Orii, Hideki Ota, Masanobu Niiyama, Ryoichi Tanaka, Yoshihiro Morino, Kunihiro Yoshioka
journal or publication title	Journal of cardiovascular computed tomography
volume	13
number	2
page range	134-141
year	2019-04
URL	http://hdl.handle.net/10097/00130797

doi: 10.1016/j.jcct.2018.10.027

Manuscript Details

Manuscript number	JCCT_2018_27_R1
Title	Optimized Interpretation of Fractional Flow Reserve Derived from Computed Tomography: Comparison of Three Interpretation Methods
Article type	Research Paper

Abstract

Background: An optimal system for interpreting fractional flow reserve (FFR) values derived from CT (FFRCT) is lacking. We sought to evaluate performance of three FFRCT measurements in detecting ischemia by comparing them with invasive FFR. Methods: For 73 vessels in 50 patients who underwent coronary CT angiography (CCTA) and FFRCT analysis followed by invasive FFR, the greatest diameter stenosis on CCTA, FFRCT difference between distal and proximal to the stenosis (ΔFFRCT), FFRCT 2 cm distal to the stenosis (lesion-specific FFRCT), and the lowest FFRCT in distal vessel tip were calculated. Significant obstruction (≥50% diameter stenosis) and ischemia (lesion-specific FFRCT ≤0.80, the lowest FFRCT ≤0.80, or ΔFFRCT ≥0.12 based on the greatest Youden index) were compared with invasive FFR (≤0.80). Results: Forty (55%) vessels demonstrated ischemia during invasive FFR. On multivariable generalized estimating equations, ΔFFRCT (odds ratio [OR] 10.2, p<0.01) remained a predictor of ischemia over CCTA (OR 2.9), lesion-specific FFRCT (OR 3.1), and the lowest FFRCT (OR 0.9) (p>0.05 for all). Area under the curve (AUC) of ΔFFRCT (0.86) was higher than CCTA (0.66), lesion-specific FFRCT (0.71), and the lowest FFRCT (0.65) (p<0.01 for all). Addition of each FFRCT measure to CCTA showed improvement of AUC and significant net reclassification improvement (NRI): ΔFFRCT (AUC 0.84, NRI 1.24); lesion-specific FFRCT (AUC 0.77, NRI 0.83); and the lowest FFRCT (AUC 0.76, NRI 0.59) (p<0.01 for all). Conclusions: Compared with diameter stenosis, ΔFFRCT, lesion-specific FFRCT, and the lowest FFRCT improved ischemia discrimination and reclassification, with ΔFFRCT being superior in identifying and discriminating ischemia.

Keywords	coronary artery disease; fractional flow reserve; coronary computed tomography angiography; fractional flow reserve derived from computed tomography.
Taxonomy	Atherosclerosis, Computed Tomography

Corresponding Author	Hidenobu Takagi
Corresponding Author's Institution	Iwate Medical University
Order of Authors	Hidenobu Takagi, Yu Ishikawa, Makoto Orii, Hideki Ota, Masanobu Niiyama, Ryoichi Tanaka, Yoshihiro Morino, Kunihiro Yoshioka
Suggested reviewers	Charles Taylor, Jonathon Leipsic, Shaw Hua (Anthony) Kueh

Abbreviations

AUC = area under the curve

CI = confidence interval

CCTA = coronary computed tomography angiography

FFR = fractional flow reserve

FFR_{CT} = fractional flow reserve derived from coronary computed tomography angiography

ICA = invasive coronary angiography

NPV = negative predictive value

PPV = positive predictive value

ROC = receiver operating characteristics

Subdivision

1. **Introduction**

2. **Methods**

   2.1. **Study design and population**

   2.2. **CT acquisition and interpretation**

   2.3. **FFR_{CT} analysis**

   2.4. **ICA and FFR measurements**

   2.5. **Statistical analysis**

3. **Results**

   3.1. **Study population and characteristics**

   3.2. **Discrimination of ischemia**

   3.3. **Diagnosis of ischemia**

   3.4. **Additive values of FFR_{CT} parameters**

   3.5. **Relationship between FFR_{CT} parameters and stenosis grading**

   3.6. **Interobserver reproducibility**

4. **Discussion**

5. **Conclusions**

1. Introduction

Fractional flow reserve (FFR) is currently considered as the gold standard for the assessment of ischemia and guides the revascularization in patients with stable coronary artery disease.[1,2] The application of computational fluid dynamics to coronary computed tomography angiography (CCTA) enables noninvasive FFR measurement without hyperemia, which provides information on FFR along the entire coronary artery based on CCTA data sets.[3] Recently, large accuracy and clinical utility studies have validated the FFR derived from CCTA (FFR_{CT}).[4–8]

However, in the clinical setting, it is uncertain how physicians should interpret the FFR_{CT} results. In the accuracy trials, diagnostic performance has been determined through a comparison of single measurements at specified locations within the coronary artery corresponding to the location of FFR pressure wire sensor between FFR_{CT} and invasive FFR.[4–6] The data set of FFR_{CT} can provide FFR values along the entire course of the epicardial coronary arteries. Due to a gradual decrease in the FFR_{CT} value even without a focal stenosis, different

measurement locations for FFR_{CT} and invasive FFR will produce a different diagnosis, if the respective values are discordant regarding the defined threshold for ischemia of 0.80. Invasive coronary angiography (ICA) and FFR are generally downstream tests of CCTA and FFR_{CT} analyses. Thus, when physicians interpret FFR_{CT} results, they cannot apply the position where invasive FFR is measured to FFR_{CT}, and reported FFR_{CT} values may not reflect the precise location of the FFR pressure wire sensor. Therefore, an interpretation method for FFR_{CT} results is required in the clinical setting. The lowest FFR_{CT} is the value at the distal end of the coronary vessel, which is commonly used in clinical trials.[9–11] Kueh reported that lesion-specific FFR_{CT}, defined as the value within 2 cm distal to the greatest stenotic lesion, could effectively reclassify the positive result in the lowest FFR_{CT}.[12]

During invasive FFR, a pullback of the pressure wire is usually performed, with the jump-up of coronary pressure and FFR across the stenosis observed. If coronary stenosis is more severe, pressure gradient across the stenosis becomes higher. Thus, considering pressure gradients across the hemodynamically

significant stenosis, we hypothesized that a difference of FFR_{CT} value between distal and proximal to an anatomical stenosis with the greatest diameter stenosis (ΔFFR_{CT}) could become a predictor for ischemia. In this study, we investigated discrimination power, diagnostic performance, and reclassification ability of ΔFFR_{CT}, lesion-specific $FFR_{CT,}$ and the lowest FFR_{CT} for the detection of ischemia compared with invasive FFR as the reference standard.

2. Methods

2.1. Study design and population

This retrospective single-center study was approved by an institutional review board, and included patients from a prospective registry assessing the diagnostic value of noninvasive FFR_{CT} in coronary care (ADVANCE registry, ClinicalTrials.gov #NCT02499679).[13] We obtained written informed consent for the registry from all participants, and the institutional review board waived the requirement of additional informed consent for this sub-analyses. Table S1 (supplementary material) provides

inclusion and exclusion criteria for the registry. Consecutive participants in the prospective registry who underwent CCTA with FFR_{CT} analysis followed by invasive FFR measurement in our institution between September 2015 and September 2017 were included. Patients were excluded if they had prior coronary artery bypass graft surgery or percutaneous coronary intervention.

2.2. CT acquisition and interpretation

All patients underwent coronary CT calcium scoring and angiography,[14] using the following CT scanners: 0.5 mm × 320-row detector CT scanner (Aquilion ONE ViSION or Genesis Edition, Canon Medical Systems, Otawara, Japan), 0.25 mm × 128-row (TSX-304R, Canon Medical Systems) or 0.25 mm × 160-row (Aquilion Precision, Canon Medical Systems) ultra-high-resolution CT scanner.[15] Patient preparation and CT scanning were performed based on the Society of Cardiovascular Computed Tomography (SCCT) guidelines.[16,17] All patients took nitroglycerin. Patients with a heart rate of 65 beats/min received intravenous beta-blockers 5–7 min before CCTA scan. All CCTA procedures were performed with a

prospective electrocardiogram-gated scan. The detailed CCTA protocol is summarized in Table S2 (supplementary material). The optimal stationary cardiac phase with minimum motion-free datasets was determined by cardiovascular CT technologists. Both the volumetric CT dose index and dose-length product were recorded for each patient. The corresponding effective radiation dose was calculated using a conversion factor of 0.014 mSv/mGy·cm.[18] Coronary stenosis severity was assessed by radiologists with more than 20 years experience (RT and KY) using a commercially available workstation (Ziostation2, Ziosoft, Tokyo, Japan). The degree of coronary stenosis was graded as minimal (<25%), mild (25%–49%), moderate (50%–69%), and severe (70%–99%) according to the SCCT guideline.[19] Significant obstruction was defined as luminal stenosis of ≥50%.

2.3. FFR_{CT} analysis

FFR_{CT} analysis was blindedly and independently performed at HeartFlow Inc., Redwood City, CA, USA. The results provide FFR_{CT} value throughout the coronary arterial tree. For each coronary artery, a radiologist (HT with 7 years experience)

calculated three parameters as follows: a difference of FFR_{CT} values between distal and proximal to an anatomical stenosis with greatest stenosis on the coronary vessel (ΔFFR_{CT}), FFR_{CT} value within 2 cm distal to the tightest point (lesion-specific FFR_{CT}), and the lowest FFR_{CT} value in the distal vessel tip (the lowest FFR_{CT}) (Figure 1). Figure 2 shows a detailed method on how to obtain the ΔFFR_{CT}. For lesion-specific FFR_{CT}, the tightest point similar to that employed in ΔFFR_{CT} was used, and the position 2 cm distal to the location was measured on a curved planar reconstructed image. When serial lesions were observed, only the lesion with greatest diameter stenosis was used, and the value was measured strictly at 2 cm distal to the tightest point regardless of the presence or absence of plaque. If lesion-specific FFR_{CT} was distal to the distal vessel tip on FFR_{CT}, values in the distal tip were employed as the lesion-specific FFR_{CT} (i.e. lesion-specific FFR_{CT} = the lowest FFR_{CT}). Given that FFR_{CT} does not provide a value of less than 0.50, the value of <0.50 was defined as 0.50. Ischemia was defined as an FFR_{CT} value of ≤0.80 for lesion-specific FFR_{CT} and the lowest FFR_{CT}. To assess interobserver

reproducibility, another radiologist (MO with 10 years experience) independently and blindly calculated these FFR_{CT} measures for consecutive 30 vessels. The optimal threshold value of ΔFFR_{CT} was defined as values corresponding to the maximum Youden index in the receiver operating characteristic (ROC) curve.[20]

2.4. ICA and FFR measurements

Cardiologists performed ICA and FFR on a biplane angiography system. FFR was performed with a 0.014-inch pressure monitoring wire (PressureWire Aeris, St. Jude Medical Systems, USA). Hyperemia was attained after administration of intravenous adenosine triphosphate (140 μg/kg/min, n = 37) or intracoronary nicorandil (2 mg, n = 13). FFR was calculated automatically by dividing the mean distal coronary pressure by the mean aortic pressure during hyperemia. The position of the distal pressure sensor was recorded, and compared with 2 cm distal to the tightest point (i.e. position of lesion-specific FFR_{CT}) and the distal end of FFR_{CT} (i.e. position of the lowest FFR_{CT}) (Figure 3). FFR was considered diagnostic of ischemia at a threshold of ≤0.80.

2.5. Statistical analysis

No power analysis was performed because of the lack of previous studies on the topic. Descriptive statistics were presented as mean ± standard deviation (SD) for normally distributed variables (Shapiro-Wilk test, $p \geq 0.05$), as medians with interquartile ranges for non-normally distributed variables, and as numbers of cases (and percentages) per group for categorical variables. The interobserver reproducibilities were assessed using intraclass correlation coefficients (ICC) for absolute agreement of single measures with 95% confidence interval (CI). The per-vessel area under the curve (AUC), accuracy, sensitivity, specificity, and positive predictive (PPV) and negative predictive value (NPV) for the detection of ischemia compared with invasive FFR were calculated with 95% CI. AUC comparisons were performed as previously described by DeLong.[21] Comparisons of accuracy, sensitivity, and specificity were performed by using the Cochran's Q tests, followed by between-group comparisons using post-hoc Dunn's tests with Bonferroni correction.[22] Bootstrapping with 10,000 samples was used for adjustment for

clustering effects in the 95% CI, and for comparison of diagnostic performance. Binary logistic generalized estimating equations were used to evaluate the relationship between FFR_{CT} parameters and ischemia determined by invasive FFR, since multiple vessels per patient were counted. Additive values of each FFR_{CT} measure was evaluated by category-free net reclassification improvement (NRI).[23,24] Computations were performed using JMP Pro 12.2 (SAS Institute Inc., Cary, NC, USA), SPSS Statistics version 25 (IBM corporation, Armonk, NY, USA) or R 3.3.3 (R Foundation for Statistical Computing, Vienna, Austria) software. Two-sided $p<0.05$ indicated statistical significance.

3. Results

3.1. Study population and characteristics

Among 106 patients who underwent FFR_{CT} analysis, forty-one (39%) patients defer ICA based on CCTA/FFR_{CT} results. Fourteen patients who underwent ICA without invasive FFR measurement and one patient with history of PCI were

excluded. Consequently, this study included 73 vessels with >25% stenosis in 50 patients (1.5 vessels per patient) (Figure 4). Patient and CCTA characteristics are summarized in Table 1 and 2, respectively. Ischemia was found in 55% (40/73) of vessels of 66% (33/50) patients during invasive FFR; mean invasive FFR value was 0.76 ± 0.17. Table 3 provides details on the extent of coronary stenosis. For invasive FFR measurements, five positions of distal wire sensor were missing. In the remaining 68 vessels, the positional relationships of distal pressure sensor to measurement points for lesion-specific FFR_{CT} and the lowest FFR_{CT} were as follows: proximal, 10% (7/68) and 63% (43/68); distal, 60% (41/68) and 13% (9/68); and same position, 29% (20/68) and 24% (16/68), respectively (Figure 3).

3.2. Discrimination of ischemia

Per-vessel AUC for CCTA, ΔFFR_{CT}, lesion-specific FFR_{CT}, and the lowest FFR_{CT} were 0.66 (95% CI, 0.56–0.76), 0.86 (95% CI, 0.75–0.92), 0.71 (95% CI, 0.59–0.80), and 0.65 (95% CI, 0.55–0.74), respectively (Figure 5 A). The optimal threshold value for ΔFFR_{CT} was 0.12 based on the greatest Youden index. Table 4

provides measures of diagnostic characteristics. The AUC for ΔFFR_{CT} was higher than all the other parameters: differences in AUC for CCTA, 0.20 (95% CI, 0.09–0.30, $p<0.01$), lesion-specific FFR_{CT}, 0.15 (95% CI, 0.05–0.26, $p<0.01$), and the lowest FFR_{CT}, 0.21 (95% CI, 0.11–0.31, $p<0.01$), respectively (Figure 5 A). The specificity for ΔFFR_{CT} with threshold value of 0.12 was higher than those for CCTA and the lowest FFR_{CT} (adjusted $p<0.01$ for both). The accuracy and sensitivity showed no statistical significance between CCTA, ΔFFR_{CT}, lesion-specific FFR_{CT} and, the lowest FFR_{CT} (accuracy, $p = 0.126$; and sensitivity, $p = 0.059$, respectively by Cochran's Q test). Figure 6 displays a representative case of patients with a positive result for the lowest FFR_{CT} without ischemia for the invasive FFR.

3.3. Diagnosis of ischemia

On univariable generalized estimating equations, CCTA (X^2, 6.8, odds radio [OR], 8.0 [95% CI, 1.7–38.4], $p<0.01$), ΔFFR_{CT} (X^2, 21.2, OR, 18.0 [95% CI, 5.3–61.2], $p<0.01$), lesion-specific FFR_{CT} (X^2, 10.6, OR, 6.0 [95% CI, 2.0–17.8], $p<0.01$), and the lowest FFR_{CT} (X^2, 7.7, OR, 5.9 [95% CI, 1.8–20.4], $p = 0.018$) were related

to the ischemia determined by invasive FFR (Table S3, supplementary material). On multivariable generalized estimating equation, ΔFFR_{CT} (X^2, 12.3, OR, 10.2 [95% CI, 2.8–37.3], p<0.01) remained a predictor over CCTA (X^2, 1.1, OR, 2.9 [95% CI, 0.4–21.8], p = 0.30), lesion-specific FFR_{CT}, (X^2, 2.9, OR, 3.1 [95% CI, 0.8–11.1], p = 0.091), and the lowest FFR_{CT} (X^2, 0.01, OR, 0.9 [95% CI, 0.2–5.1], p = 0.95) (Table S3, supplementary material).

3.4. Additive values of FFR_{CT} parameters

All diagnostic models using CCTA and FFR_{CT} measures demonstrated higher AUC than the model with CCTA alone (CCTA alone, 0.66 [95% CI, 0.56–0.75]; CCTA + ΔFFR_{CT}, 0.84 [95% CI, 0.73–0.91]; CCTA + lesion-specific FFR_{CT}, 0.77 [95% CI, 0.65–0.86]; and CCTA + the lowest FFR_{CT}, 076 [95% CI, 0.65–0.85], p<0.01 for all) (Figure 5 B, C, and D). All FFR_{CT} parameters enabled effective reclassification of CCTA diameter stenosis as follows: ΔFFR_{CT} (NRI, 1.24 [95% CI, 0.87–1.60], p<0.01); lesion-specific FFR_{CT} (NRI, 0.83 [95% CI, 0.40–1.25], p<0.01); and the lowest FFR_{CT} (NRI, 0.59 [95% CI, 0.21–0.97], p<0.01).

3.5. Relationship between FFR_{CT} parameters and stenosis grading

The relationships between FFR_{CT} measures and anatomical stenosis determined by CCTA are displayed in Figure 7. All 20 vessels with severe (70%–99%) stenosis demonstrated hemodynamic significance on invasive FFR. Vessels with mild (25%–49%) and moderate (50%–69%) stenoses included 19% (3/16) and 46% (17/37), respectively, of vessels with ischemia. For the 37 moderate stenotic lesions, ΔFFR_{CT}, lesion-specific FFR_{CT} and the lowest FFR_{CT} correctly reclassified 43% (16/37), 32% (12/37), and 24% (9/37), respectively, of vessels into the non-ischemia (invasive FFR >0.80). For the remaining 16 vessels with mild stenotic lesions, ΔFFR_{CT} could not reclassify into the ischemia (invasive FFR ≤0.80), while lesion-specific FFR_{CT}, and the lowest FFR_{CT} correctly reclassified 13% (2/16) and 13% (2/16) of vessels, respectively into the ischemia (invasive FFR ≤0.80).

3.6. Interobserver reproducibility

For each FFR_{CT} measures, intraclass correlation coefficients were as follows: ΔFFR_{CT}, 0.90 (95% CI, 0.79–0.95); lesion-specific FFR_{CT}, 0.86 (95% CI, 0.73–

0.93); and the lowest FFR_{CT}, 1.00 (95% CI, 0.99–1.00).

4. Discussion

At present, interpreting or reporting FFR_{CT} result system in a clinical condition is lacking. We developed ΔFFR_{CT} as a predictor of ischemia, and investigated discrimination power, diagnostic accuracy and reclassification ability of ΔFFR_{CT}, lesion-specific $FFR_{CT,}$ and the lowest FFR_{CT}. Each FFR_{CT} measures showed improvement of AUC and effective reclassifications for the detection of ischemia, compared with those of CCTA alone. Among these FFR_{CT} measures, ΔFFR_{CT} showed the highest AUC, and the specificity of ΔFFR_{CT} with threshold value of 0.12 was higher compared to that of the lowest FFR_{CT}. The per-vessel sensitivity and specificity of ΔFFR_{CT} were comparable to those in the NXT trial (sensitivity and specificity of 84% and 86%, respectively).[6] Multivariable generalized estimating equation showed that ΔFFR_{CT} remained a predictor of ischemia over CCTA, lesion-specific FFR_{CT}, and the lowest FFR_{CT}. Furthermore, these FFR_{CT} measures could

efficiently reclassify moderate stenotic lesions and be limited to vessels with mild or severe stenosis. Combined with anatomical stenosis evaluation, ΔFFR_{CT}, lesion-specific FFR_{CT}, and the lowest FFR_{CT} will aid in the diagnosis of ischemia. Moreover, from the perspective of clinical use, the advantage of these parameters is that the measurement is not based on the position of the pressure wire sensor. Thus, these FFR_{CT} measurements, which are intended for clinical use, will enhance the clinical value of FFR_{CT} when managing patients with suspected ischemia.

However, in our study, more than half (63%) of invasive FFR measurements were performed proximal to the lowest FFR_{CT}, whereas 60% were performed distal to the lesion-specific FFR_{CT}. Considering that there is a gradual decrease in the FFR_{CT} value even without a focal stenosis, positional differences could cause discordances in values between FFR_{CT} and invasive FFR. If the same threshold value of 0.80 for ischemia is used, the lowest FFR_{CT} could overestimate the severity of the lesion compared with invasive FFR, whereas lesion-specific FFR_{CT} could underestimate the severity. Thus, these measurements do not precisely reflect

invasive FFR results, and simply reporting the lowest FFR_{CT} or lesion-specific FFR_{CT} alone can confuse rather than help in clinical decision-making when considering referral for ICA. Especially, the AUC (0.65) and specificity (39%) of the lowest FFR_{CT} were modest, which probably account for the disagreement of the measurement location. The lowest FFR_{CT} might have a tendency to become lower than those measured at the proximal to the distal vessel tip. These results indicate that simply using the lowest FFR_{CT} is unreliable, and a system for interpreting FFR_{CT} results should be reconsidered in clinical settings.

Our study has some limitations. It is a single-center study with a small sample size. Moreover, although this study included patients from the prospective registry, this subanalysis is not prespecified. Additionally, the population consisted of patients who underwent invasive ICA and FFR, which causes a potential selection bias of patients referred for FFR_{CT} evaluation and those subsequently referred for ICA and FFR. Patients who had previously undergone revascularization were also excluded from the study. Thus, the usefulness of FFR_{CT} parameters warrants

further investigation. Furthermore, this study lacks clinical outcome data, such as reduction of unnecessary ICA or adverse cardiac events. For those reasons, we could just conclude that ΔFFR_{CT}, lesion-specific FFR_{CT}, and the lowest FFR_{CT} will help in interpreting FFR_{CT} results in patients referred for ICA and invasive FFR measurement. To show the usefulness of these methods, a further clinical outcome study is needed.

5. Conclusions

Although FFR_{CT} is a clinically useful diagnostic tool, a standardized interpretation system is lacking in clinical settings. Adding ΔFFR_{CT}, lesion-specific FFR_{CT}, and the lowest FFR_{CT} to the diameter stenosis determined by CCTA showed improvements in discriminating and effectively reclassifying ischemia, with ΔFFR_{CT} being superior in identifying and discriminating ischemia. In contrast, the lowest FFR_{CT} was of limited value, which suggests that positional difference between FFR_{CT} and invasive FFR may have a potential harm; thus, cautious clinical

interpretation of FFR_{CT} values is crucial.

Acknowledgement.

The authors acknowledge members of the Division of Cardiovascular Radiology and Division of Cardiology for kind support to this study.

Funding Sources

This work was supported by Grant-in-Aid for Young Scientists (B) from the Japan Society for the Promotion of Science (JSPS KAKENHI) [Grant Number, 17K18044]; and Program for the Private University Research Branding Project from the Ministry of Education, Culture, Sports, Science and Technology (MEXT). ADVANCE registry was supported by HeartFlow, Inc., Redwood City, CA, USA.

References

1. Fihn SD, Gardin JM, Abrams J, et al. 2012 ACCF/AHA/ACP/AATS/PCNA/SCAI/STS Guideline for the Diagnosis and Management of Patients With Stable Ischemic Heart Disease: A Report of the American College of Cardiology Foundation/American Heart Association Task Force on Practice Guidelines, and the American College of Physicians, American Association for Thoracic Surgery, Preventive Cardiovascular Nurses Association, Society for Cardiovascular Angiography and Interventions, and Society of Thoracic Surgeons. *Circulation*. 2012;126(25):e354-e471. doi:10.1161/CIR.0b013e318277d6a0
2. Windecker S, Kolh P, Alfonso F, et al. 2014 ESC/EACTS Guidelines on myocardial revascularization: The Task Force on Myocardial Revascularization of the European Society of Cardiology (ESC) and the European Association for Cardio-Thoracic Surgery (EACTS)Developed with the special contribution of the European Association of Percutaneous Cardiovascular Interventions (EAPCI). *Eur Heart J*. 2014;35(37):2541-2619. doi:10.1093/eurheartj/ehu278
3. Taylor CA, Fonte TA, Min JK. Computational Fluid Dynamics Applied to Cardiac Computed Tomography for Noninvasive Quantification of Fractional Flow Reserve. *J Am Coll Cardiol*. 2013;61(22):2233-2241. doi:10.1016/j.jacc.2012.11.083
4. Koo B-K, Erglis A, Doh J-H, et al. Diagnosis of Ischemia-Causing Coronary Stenoses by Noninvasive Fractional Flow Reserve Computed From Coronary Computed Tomographic Angiograms: Results From the Prospective Multicenter DISCOVER-FLOW (Diagnosis of Ischemia-Causing Stenoses Obtained Via Noninvasive Fractional Flow Reserve) Study. *J Am Coll Cardiol*. 2011;58(19):1989-1997. doi:10.1016/j.jacc.2011.06.066
5. Min JK, Leipsic J, Pencina MJ, et al. Diagnostic Accuracy of Fractional Flow Reserve From Anatomic CT Angiography. *JAMA*. 2012;308(12):1237.

doi:10.1001/2012.jama.11274

6. Nørgaard BL, Leipsic J, Gaur S, et al. Diagnostic Performance of Noninvasive Fractional Flow Reserve Derived From Coronary Computed Tomography Angiography in Suspected Coronary Artery Disease. *J Am Coll Cardiol*. 2014;63(12):1145-1155. doi:10.1016/j.jacc.2013.11.043
7. Douglas PS, Pontone G, Hlatky MA, et al. Clinical outcomes of fractional flow reserve by computed tomographic angiography-guided diagnostic strategies vs. usual care in patients with suspected coronary artery disease: the prospective longitudinal trial of FFRCT: outcome and resource impacts study. *Eur Heart J*. 2015;36(47):3359-3367. doi:10.1093/eurheartj/ehv444
8. Douglas PS, De Bruyne B, Pontone G, et al. 1-Year Outcomes of FFRCT-Guided Care in Patients With Suspected Coronary Disease. *J Am Coll Cardiol*. 2016;68(5):435-445. doi:10.1016/j.jacc.2016.05.057
9. Kitabata H, Leipsic J, Patel MR, et al. Incidence and predictors of lesion-specific ischemia by FFR CT : Learnings from the international ADVANCE registry. *J Cardiovasc Comput Tomogr*. 2018;12(2):95-100. doi:10.1016/j.jcct.2018.01.008
10. Sand NPR, Veien KT, Nielsen SS, et al. PRrospEctive Comparison of FFR Derived From Coronary CT Angiography With SPECT PerfuSion Imaging in Stable Coronary ArtEry DiSeaSe. *JACC Cardiovasc Imaging*. June 2018. doi:10.1016/j.jcmg.2018.05.004
11. Fairbairn TA, Nieman K, Akasaka T, et al. Real-world clinical utility and impact on clinical decision-making of coronary computed tomography angiography-derived fractional flow reserve: lessons from the ADVANCE Registry. *Eur Heart J*. August 2018. doi:10.1093/eurheartj/ehy530
12. Kueh SH, Mooney J, Ohana M, et al. Fractional flow reserve derived from coronary computed tomography angiography reclassification rate using value distal to lesion compared to lowest value. *J Cardiovasc Comput Tomogr*. September 2017. doi:10.1016/j.jcct.2017.09.009
13. Chinnaiyan KM, Akasaka T, Amano T, et al. Rationale, design and goals of the

HeartFlow assessing diagnostic value of non-invasive FFRCT in Coronary Care (ADVANCE) registry. *J Cardiovasc Comput Tomogr*. December 2016. doi:10.1016/j.jcct.2016.12.002

14. Agatston AS, Janowitz WR, Hildner FJ, Zusmer NR, Viamonte M, Detrano R. Quantification of coronary artery calcium using ultrafast computed tomography. *J Am Coll Cardiol*. 1990;15(4):827-832. doi:10.1016/0735-1097(90)90282-T
15. Takagi H, Ryoichi Tanaka, Kyohei Nagata, et al. Diagnostic performance of coronary CT angiography with ultra-high-resolution CT: Comparison with invasive coronary angiography. *Eur J Radiol*. 2018;101:30-37. doi:10.1016/j.ejrad.2018.01.030
16. Abbara S, Arbab-Zadeh A, Callister TQ, et al. SCCT guidelines for performance of coronary computed tomographic angiography: A report of the Society of Cardiovascular Computed Tomography Guidelines Committee. *J Cardiovasc Comput Tomogr*. 2009;3(3):190-204. doi:10.1016/j.jcct.2009.03.004
17. Abbara S, Blanke P, Maroules CD, et al. SCCT guidelines for the performance and acquisition of coronary computed tomographic angiography: A report of the society of Cardiovascular Computed Tomography Guidelines Committee. *J Cardiovasc Comput Tomogr*. 2016;10(6):435-449. doi:10.1016/j.jcct.2016.10.002
18. Hausleiter J, Meyer T, Hermann F, et al. Estimated radiation dose associated with cardiac CT angiography. *JAMA*. 2009;301(5):500–507.
19. Leipsic J, Abbara S, Achenbach S, et al. SCCT guidelines for the interpretation and reporting of coronary CT angiography: A report of the Society of Cardiovascular Computed Tomography Guidelines Committee. *J Cardiovasc Comput Tomogr*. 2014;8(5):342-358. doi:10.1016/j.jcct.2014.07.003
20. Youden WJ. Index for rating diagnostic tests. *Cancer*. 1950;3(1):32-35.
21. DeLong ER, DeLong DM, Clarke-Pearson DL. Comparing the areas under two or more correlated receiver operating characteristic curves: a nonparametric

approach. *Biometrics*. 1988;44(3):837-845.
22. Dunn OJ. Multiple Comparisons Using Rank Sums. *Technometrics*. 1964;6(3):241-252. doi:10.2307/1266041
23. Pencina MJ, D' Agostino RB, D' Agostino RB, Vasan RS. Evaluating the added predictive ability of a new marker: From area under the ROC curve to reclassification and beyond. *Stat Med*. 2008;27(2):157-172. doi:10.1002/sim.2929
24. Cook NR, Paynter NP. Performance of reclassification statistics in comparing risk prediction models. *Biom J*. 2011;53(2):237-258. doi:10.1002/bimj.201000078
25. Cury RC, Abbara S, Achenbach S, et al. CAD-RADSTM Coronary Artery Disease – Reporting and Data System. An expert consensus document of the Society of Cardiovascular Computed Tomography (SCCT), the American College of Radiology (ACR) and the North American Society for Cardiovascular Imaging (NASCI). Endorsed by the American College of Cardiology. *J Cardiovasc Comput Tomogr*. 2016;10(4):269-281. doi:10.1016/j.jcct.2016.04.005

Figure legends

Figure 1 – Quantitative parameters derived from FFR_{CT}.

ΔFFR_{CT} was calculated as the difference of values in proximal and distal sites, which were manually selected to be the most adjacent points to the maximal stenosis in which there was minimal or no plaque. Lesion-specific FFR_{CT} was defined as the value at 2 cm distal to the maximal stenosis. The lowest FFR_{CT} was the value at the distal end of the coronary vessel in FFR_{CT}.

FFR_{CT} = fractional flow reserve derived from computed tomography.

Figure 2 – Detailed methods in obtaining ΔFFR_{CT}.

We obtained ΔFFR_{CT} using the following 3 steps (A): (1) we identified the greatest stenosis in the coronary tree; (2) selected proximal and distal adjacent points to the tightest point in which there is minimal or no plaque; (3) and subtracted $FFR_{CTdistal}$ from $FFR_{CTproximal}$, where $FFR_{CTproximal}$ and $FFR_{CTdistal}$ were defined as FFR_{CT} values at the proximal and distal points, respectively. If there was a diffuse plaque (B), we

selected the proximal or distal points for ΔFFR_{CT} far from the tightest point (arrow head), and the distance between proximal or distal points became longer. In a case with serial lesions (C), we strictly selected proximal and distal points adjacent to the tightest point (arrow head) in which there is minimal or no plaque, independently of other stenosis severity.

FFR_{CT} = fractional flow reserve derived from computed tomography

Figure 3 – Positional relationship of the pressure wire sensor to the lesion-specific FFR_{CT} and the lowest FFR_{CT}.

The position of the distal pressure sensor (star) was compared with the position 2 cm distal to the tightest point (i.e. position of lesion-specific FFR_{CT}) (circle) or that at the distal end of FFR_{CT} (i.e. position of the lowest FFR_{CT}) (triangle). A shows a pressure sensor positioned proximal to the lesion-specific FFR_{CT} and the lowest FFR_{CT}, whereas B and C show a sensor positioned between lesion-specific FFR_{CT} and the lowest FFR_{CT}, and distal to both, respectively. In our study, five positions of

distal wire sensor were missing. In the remaining 68 vessels, the positional relationships of distal pressure sensor to measurement points for lesion-specific FFR_{CT} (D) and the lowest FFR_{CT} (E) were as follows: proximal, 10% (7/68) and 63% (43/68); distal, 60% (41/68) and 13% (9/68); and same position, 29% (20/68) and 24% (16/68), respectively.

FFR_{CT} = fractional flow reserve derived from computed tomography

Figure 4 – Study enrollment.

Among 106 patients who underwent FFR_{CT} analysis, forty-one (39%) patients defer ICA based on CCTA and FFR_{CT} results. The other fourteen (13%) patients underwent ICA or revascularization without invasive FFR measurement. Consequently, fifty-one patients underwent invasive FFR. One patient with history of PCI was excluded. A total of 73 vessels in 50 patients were analyzed.

FFR_{CT} = fractional flow reserve derived from computed tomography, ICA = invasive coronary angiography, FFR = fractional flow reserve, and PCI = percutaneous

coronary intervention.

Figure 5 – Receiver operating characteristic (ROC) curves of CCTA, ΔFFR_{CT}, lesion-specific FFR_{CT}, and the lowest FFR_{CT} in predicting ischemia (N = 73 vessels).

A shows ROC curves for predicting ischemia using CCTA, ΔFFR_{CT}, lesion-specific FFR_{CT}, and the lowest FFR_{CT}. B, C and D show the ROC curves of models using CCTA with and without ΔFFR_{CT}, lesion-specific FFR_{CT}, and the lowest FFR_{CT}, respectively. Threshold value of 0.12 corresponding to the maximum Youden index was used for the comparison between CCTA and CCTA with ΔFFR_{CT}.

*Indicates statistically significant difference between AUC for CCTA and CCTA with parameters derived from FFR_{CT} (B, C, and D) using DeLong test.[21]

CCTA = coronary computed tomography angiography, FFR_{CT} = fractional flow reserve derived from computed tomography, and AUC = area under the curve.

Figure 6 – Representative case example from a study.

A 70-year-old man with atypical chest pain. Curved planar reconstruction image of CCTA (A) shows a moderate stenosis (50%–69% diameter stenosis) in the proximal left anterior descending artery (arrow head). Although the lowest FFR_{CT} is 0.76, which suggests ischemia, ΔFFR_{CT} and lesion-specific FFR_{CT} suggest non-ischemic lesion (B). Invasive FFR measurement was performed at the proximal to the distal vessel tip of FFR_{CT} (circles), in which the value of 0.81 suggests non-ischemia (C and D).

FFR_{CT} = fractional flow reserve derived from computed tomography, and CCTA = coronary computed tomography angiography.

Figure 7 – Relationship between FFR_{CT} measures and anatomical stenosis determined by CCTA.

Distributions of ΔFFR_{CT} (A), lesion-specific FFR_{CT} (B), and the lowest FFT_{CT} (C) in each group with 25%–49%, 50%–69%, and 70%–99% diameter stenosis

determined by CCTA are shown. Box and plots show the medians, quartiles, and ranges in FFR_{CT} parameters. Individual values are also shown as a circle (invasive FFR ≤0.80) or a square (invasive FFR >0.80). Threshold values of each FFR_{CT} parameter are displayed as dashed lines. All 20 vessels with 70%–99% diameter stenosis demonstrated functional significance during invasive FFR, and vessels with 25%-49% or 50%–69% included 19% (3/16) or 54% (20/37) of vessels without ischemia, respectively.

FFR_{CT} = fractional flow reserve derived from computed tomography, and FFR = fractional flow reserve

Table 1. Patient characteristics (N = 50)

Variables	Values
Sex (woman)*	14 (7/50)
Age (years)	71 (57–75)
Height (cm)	164 (160–172)
Weight (kg)	67 (60–75)
Body mass index (kg/m^2)	26 (23–27)
Hypertension*	74 (37/50)
Diabetes*	34 (17/50)
Dyslipidemia*	62 (31/50)
Current/past smoker*	50 (25/50)
Serum creatinine (mg/dl)	0.82 (0.74–0.90)
Estimated glomerular filtration rate (ml/min/1.73m^2)	70 (62–78)

Note – Unless otherwise noted, data are medians, with quartiles in parentheses.

*Data are percentages, with raw data in parentheses.

Table 2. CT characteristics (N = 50)

Variables	Values
CT scanner	
0.5 mm × 320-row CT (Aquilion One ViSION)	24 (12/50)
0.5 mm × 320-row CT (Aquilion One GENESIS)	26 (13/50)
0.25 mm × 128-row CT (TSX-304R)	44 (22/50)
0.25 mm × 160-row CT (Aquilion Precision)	6 (3/50)
Agatston score[14]*	251 (51–531)
0–400	62 (31/50)
>400	38 (19/50)
Nitrate administrated	100 (50/50)
Beta-blocker administrated	48 (24/50)
Arrhythmia	2 (1/50)
Mean heart rate during CCTA (beats per minute)*	57 (52–61)
Dose of iodine contrast medium (ml)*	57 (45–67)

Volumetric CT dose index for CCTA (mGy)*	23 (9–31)
Dose-length product for CCTA (mGy·cm)*	329 (111–449)
Effective radiation dose for CCTA (mSv)*†	4.6 (1.6–6.3)

Note – Unless otherwise noted, data are percentages, with raw data in parentheses.

*Data are medians, with quartiles in parentheses.

†Effective radiation dose was calculated using a conversion factor of 0.014 mSv/mGy·cm.[18]

CCTA = coronary computed tomography angiography

Table 3. Extent of coronary stenosis (N = 50 patients; N = 73 vessels)

Variables	Values
Vessel with CCTA maximum stenosis of 25–49%	22 (16/73)
Vessel with CCTA maximum stenosis of 50–69%	51 (37/73)
Vessel with CCTA maximum stenosis of 70–99%	27 (20/73)
Patients with CAD-RADS 3*	38 (19/50)
Patients with CAD-RADS 4A*	52 (26/50)
Patients with CAD-RADS 4B*	6 (3/50)
Patients with CAD-RADS 5*	4 (2/50)
Vessel with FFR ≤0.80	55 (40/73)
RCA with FFR ≤0.80	57 (8/14)
LAD with FFR ≤0.80	61 (25/41)
LCX with FFR ≤0.80	35 (6/17)
Patients with FFR ≤0.80 in >1 vessel	66 (33/50)

Note – Data are percentages, with raw data in parentheses.

*All patients were graded using Coronary Artery Disease: Reporting and Data System (CAD-RADS) as previously described.[25]

CCTA = coronary computed tomography angiography, FFR = fractional flow reserve, RCA = right coronary artery, LAD = left anterior descending artery, and LCX = left circumflex.

Table 4. Per-vessel diagnostic accuracy of CCTA, ΔFFR_{CT}, lesion-specific FFR_{CT} and the lowest FFR_{CT} (N = 73).

Variables	CCTA†	ΔFFR_{CT}‡	Lesion-specific FFR_{CT}§	The lowest FFR_{CT}§
True positive*	37	32	31	36
True negative*	13	27	21	13
False positive*	20	6	12	20
False negative*	3	8	9	4
% Accuracy	69 (59–74)	81 (70–88)	71 (60–80)	67 (58–73)
% Sensitivity	93 (84–97)	80 (71–87)	78 (68–86)	90 (81–96)
% Specificity	39 (29–45)	82 (70–90)	64 (51–74)	39 (29–46)
% PPV	65 (59–68)	84 (74–91)	72 (63–80)	64 (58–68)
% NPV	81 (60–93)	77 (66–85)	70 (57–81)	77 (56–90)
AUC	0.66 (0.56–0.76)	0.86 (0.75–0.92)	0.71 (0.59–0.80)	0.65 (0.55–0.74)

Note – Unless otherwise noted, data are measures, with 95% confidence intervals.

*Data are raw data.

†For CCTA, significant obstruction was defined as diameter stenosis of ≥50%.

‡For ΔFFR_{CT}, diagnostic characteristics were calculated using the threshold value of 0.12 corresponding to the maximum Youden index.

§For lesion-specific FFR_{CT} or the lowest FFR_{CT}, functional significant was defined as FFR_{CT} value of ≤0.80.

CCTA = coronary computed tomography angiography, FFR_{CT} = fractional flow reserve derived from computed tomography, AUC = area under the curve, NPV = negative predictive value, and PPV = positive predictive value.

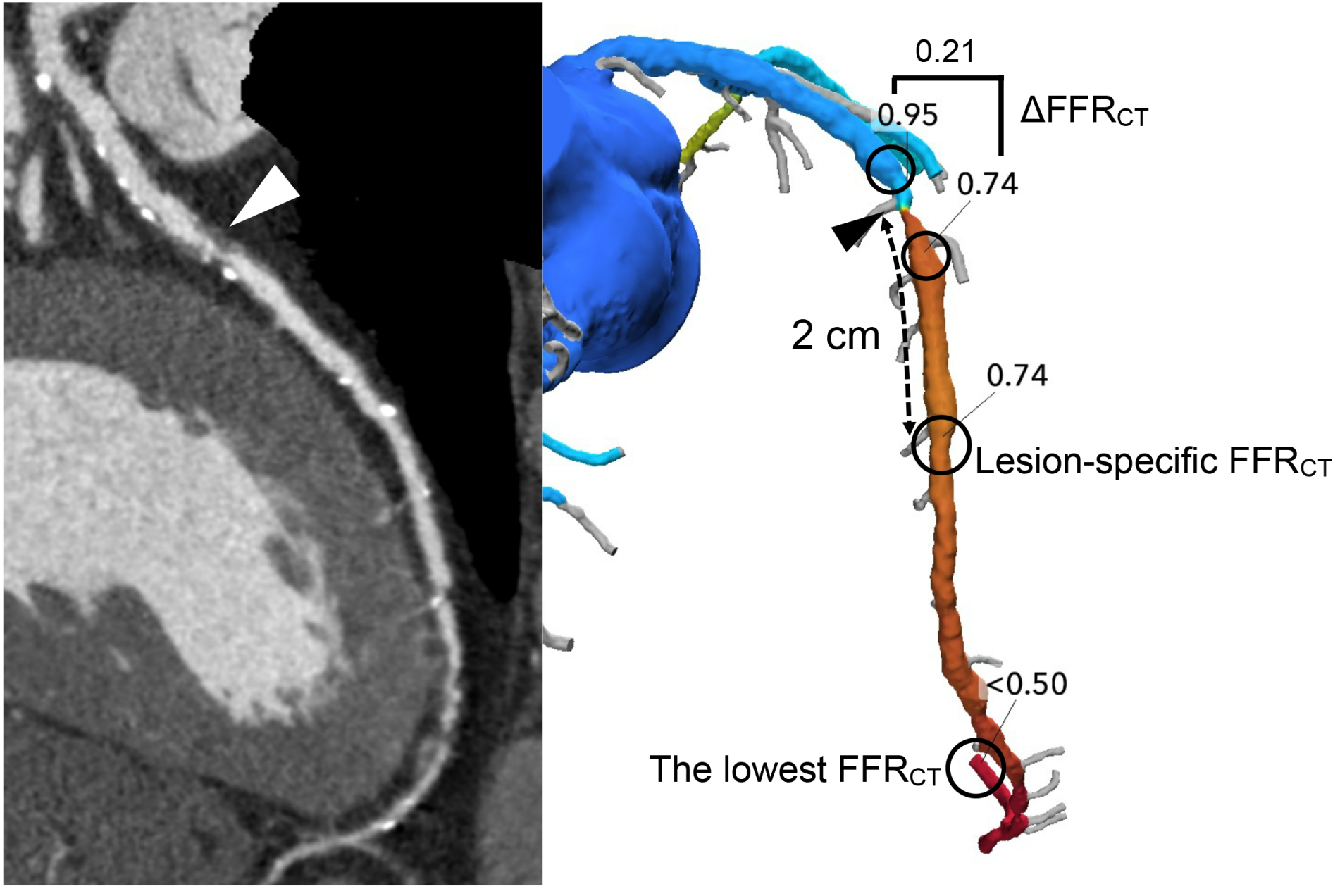
0.21
ΔFFR$_{CT}$
0.95
0.74
2 cm
0.74
Lesion-specific FFR$_{CT}$
<0.50
The lowest FFR$_{CT}$

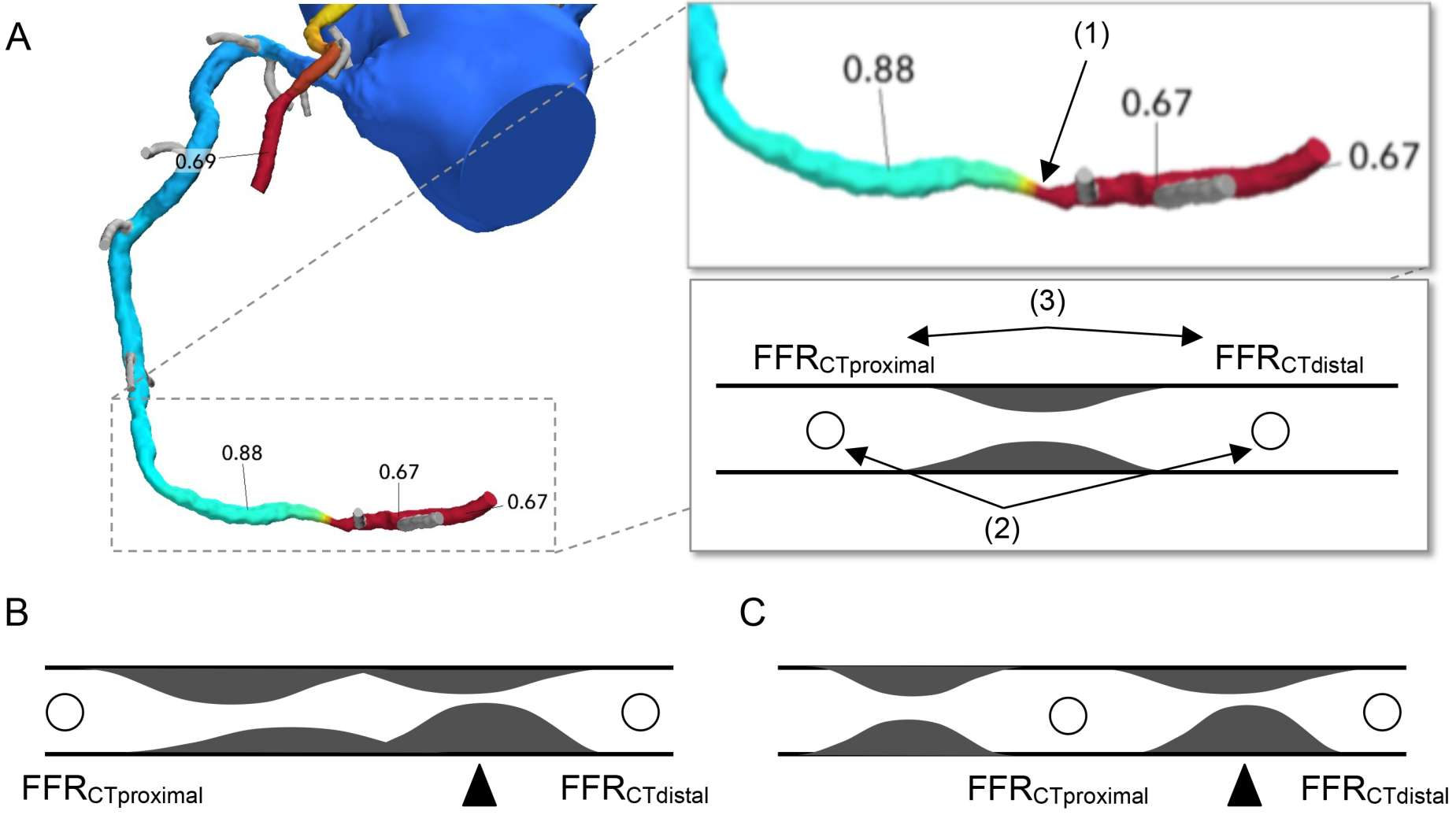
A
0.69
0.88
0.67
0.67
(1)
0.88
0.67
0.67
(3)
FFRCTproximal
FFRCTdistal
(2)
B
FFRCTproximal
FFRCTdistal
C
FFRCTproximal
FFRCTdistal

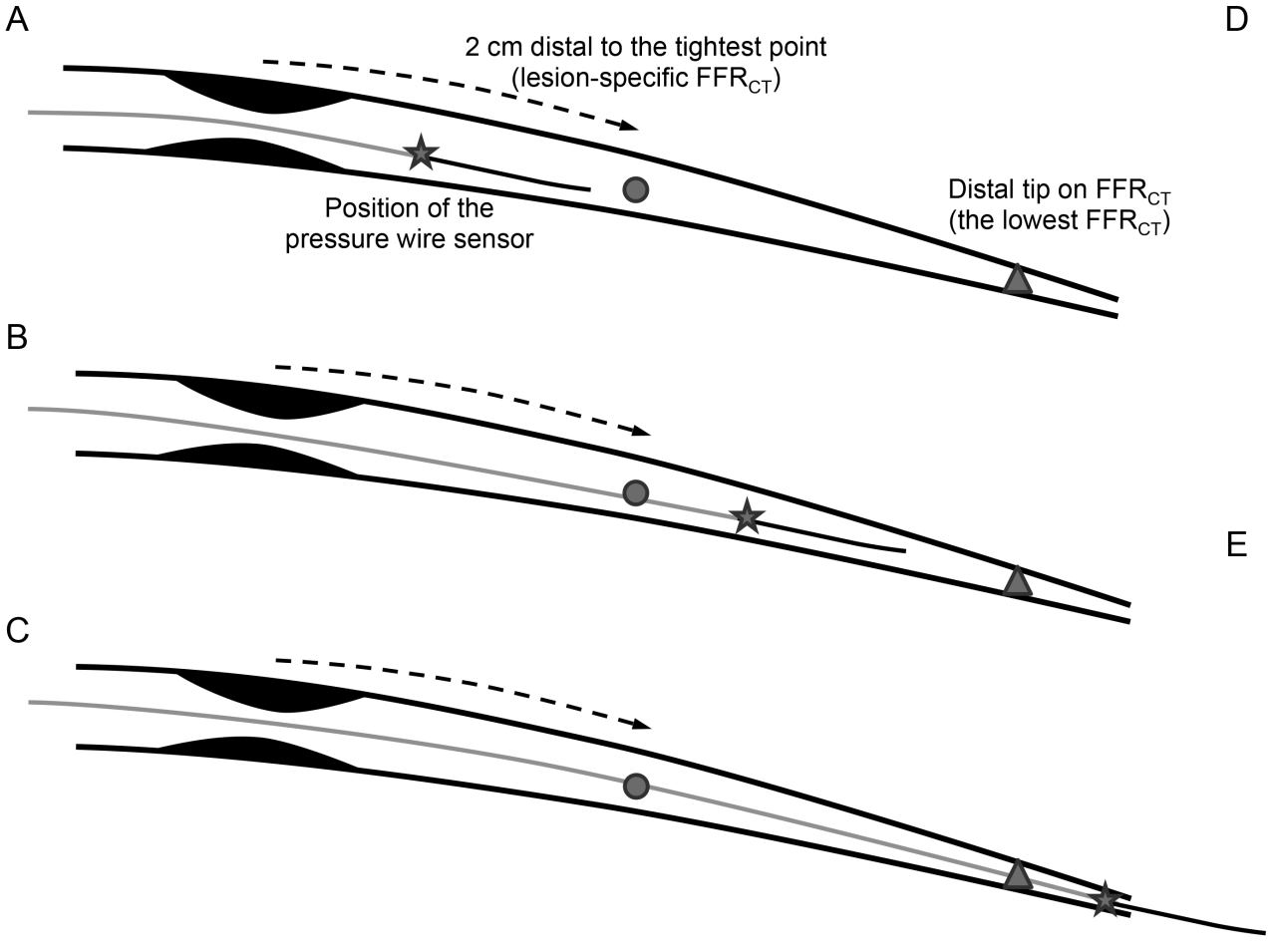
A
2 cm distal to the tightest point
(lesion-specific FFR$_{CT}$)
Position of the
pressure wire sensor
Distal tip on FFR$_{CT}$
(the lowest FFR$_{CT}$)
B
C

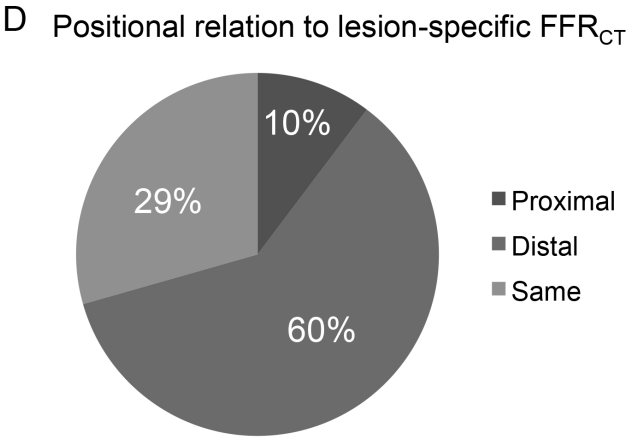
D
Positional relation to lesion-specific FFR$_{CT}$
10%
29%
60%
Proximal
Distal
Same

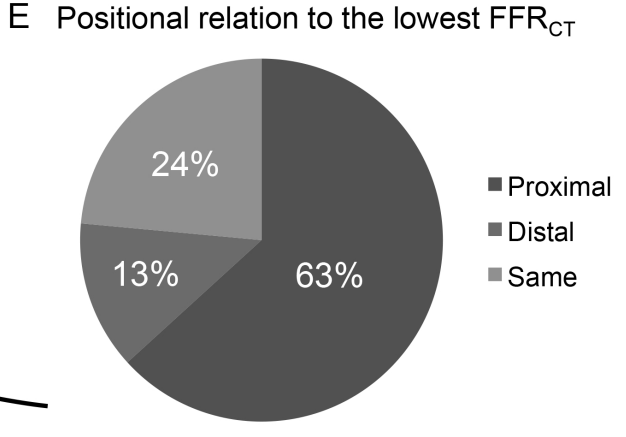
E
Positional relation to the lowest FFR$_{CT}$
24%
13%
63%
Proximal
Distal
Same

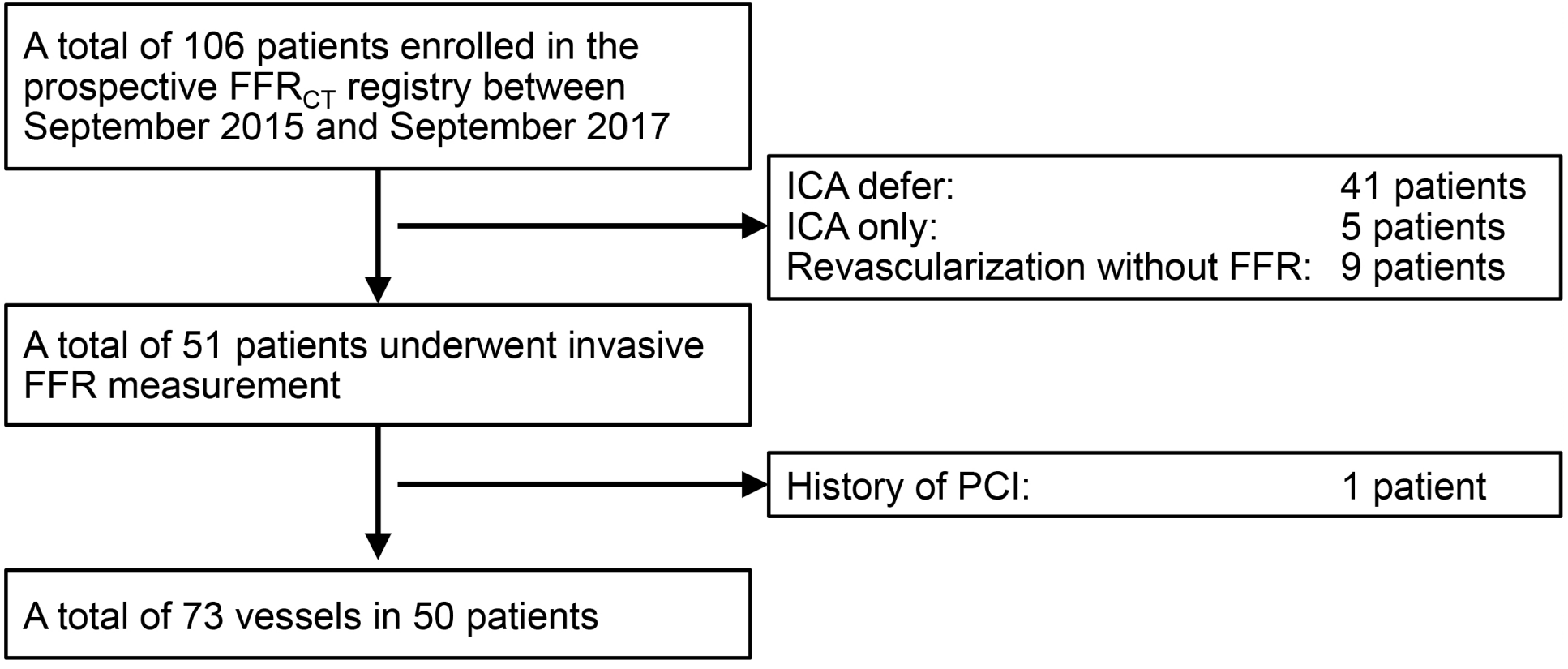
A total of 106 patients enrolled in the prospective FFR_{CT} registry between September 2015 and September 2017
ICA defer: 41 patients
ICA only: 5 patients
Revascularization without FFR: 9 patients
A total of 51 patients underwent invasive FFR measurement
History of PCI: 1 patient
A total of 73 vessels in 50 patients

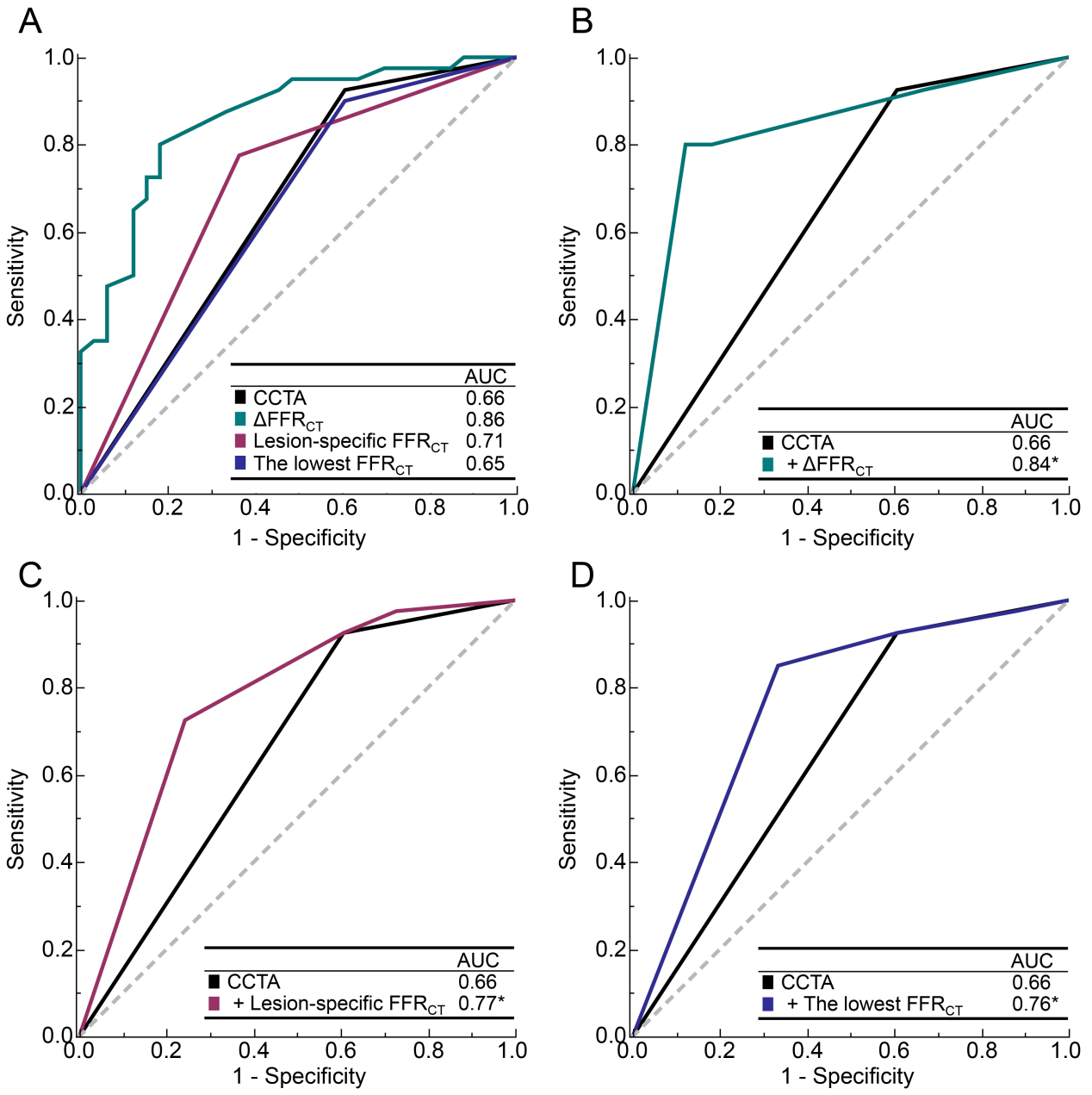
A
Sensitivity
1 - Specificity
AUC
CCTA 0.66
ΔFFR$_{CT}$ 0.86
Lesion-specific FFR$_{CT}$ 0.71
The lowest FFR$_{CT}$ 0.65
B
Sensitivity
1 - Specificity
AUC
CCTA 0.66
+ ΔFFR$_{CT}$ 0.84*
C
Sensitivity
1 - Specificity
AUC
CCTA 0.66
+ Lesion-specific FFR$_{CT}$ 0.77*
D
Sensitivity
1 - Specificity
AUC
CCTA 0.66
+ The lowest FFR$_{CT}$ 0.76*

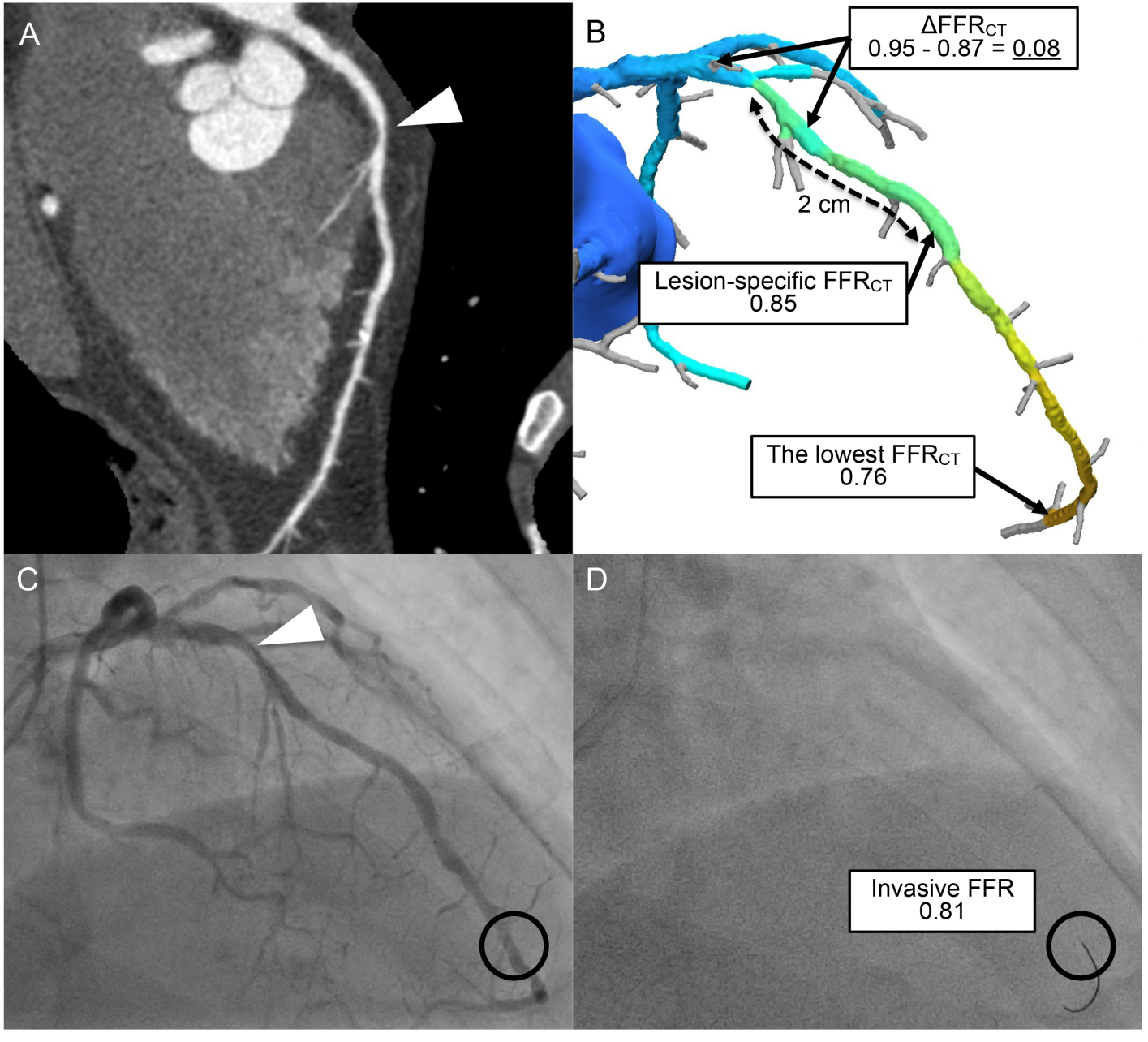
A
B
ΔFFRCT
0.95 - 0.87 = 0.08
2 cm
Lesion-specific FFRCT
0.85
The lowest FFRCT
0.76
C
D
Invasive FFR
0.81

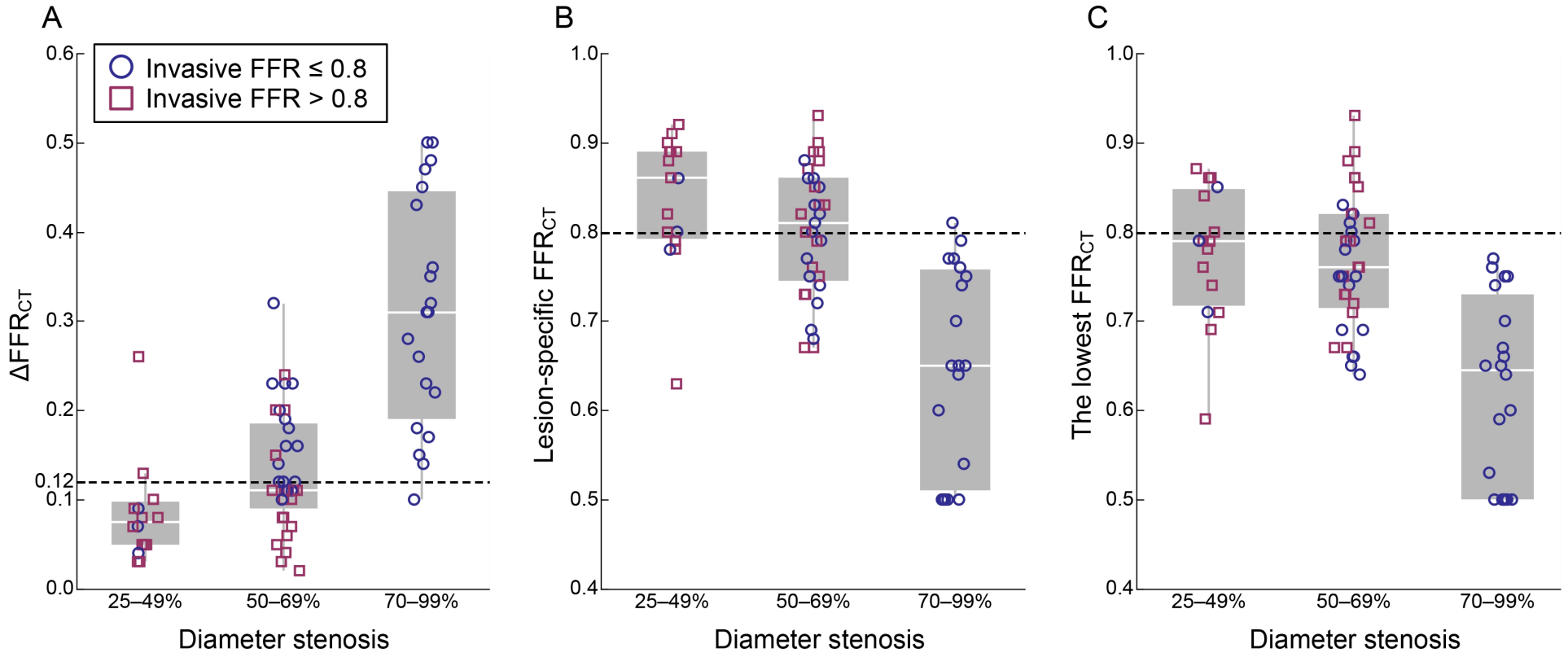
A
Invasive FFR ≤ 0.8
Invasive FFR > 0.8
ΔFFRCT
0.6
0.5
0.4
0.3
0.2
0.12
0.1
0.0
25–49%
50–69%
70–99%
Diameter stenosis
B
Lesion-specific FFRCT
1.0
0.9
0.8
0.7
0.6
0.5
0.4
25–49%
50–69%
70–99%
Diameter stenosis
C
The lowest FFRCT
1.0
0.9
0.8
0.7
0.6
0.5
0.4
25–49%
50–69%
70–99%
Diameter stenosis

Supplementary material

Table S1. Inclusion and exclusion criteria for patient enrollment of ADVANCE registry (ClinicalTrials.gov. # NCT02499679).

Inclusion
1. Provide written informed consent
2. Clinically stable, symptomatic patients who undergo cCTA and are diagnosed with CAD and meet eligibility criteria for FFR_{CT}
Exclusion
1. cCTA showing no CAD
2. Uninterpretable cCTA by site assessment, in which severe artifacts prevent angiographic evaluation
3. Any active, serious, life-threatening disease with a life expectancy of less than 1 year
4. Inability to comply with follow-up requirements

ADVANCE = Assessing Diagnostic Value of Non-invasive FFR_{CT} in Coronary Care;

FFR_{CT} = fractional flow reserve derived from computed tomography; cCTA = coronary computed tomography angiography; CAD = coronary artery disease.

Supplementary material

Table S2. Coronary CT angiography acquisition protocol.

	320-row detector CT	Ultra-high-resolution CT
CT scanner	Aquilion ONE ViSION Aquilion ONE GENESIS	TSX-304R Aquilion Precision
Scan mode	Axial	Helical
Tube voltage	120 kV or 100 kV in patients with a body mass index < 22 kg/m^2 and Agatston score[11] of < 400	
Tube current	Targeting image noise of 28 HU	
Collimation	0.5 mm x 200–280	0.25 mm x 128 (TSX-304R) or 0.25 mm x 160 (Precision)
Gantry rotation (s/rotation)	0.275	0.35
Scan RR window		
Heart rate of <70 beats/min	Diastolic phase	
Heart rate of ≥70 beats/min	Systolic to diastolic phase	
Intravenous access	A 20-gauge catheter was placed in the right antecubital vein.	
Iodine contrast medium (mgI/ml)	350 or 370	
Injection rate (ml/s)	0.07 ml/s/kg x body weight (kg)	

Injection duration (s)	10	Scan time + 5
Saline flash (ml)	35	
Scan delay	A computer-assisted bolus tracking system (SureStart, Canon Medical Systems) automatically determined. A trigger threshold was150 HU in the ROI within the ascending aorta. Subsequent to triggering, image acquisition began automatically at 5 s.	
Reconstruction field of view (mm^2)	200 x 200	
Slice thickness and increment (mm)	0.5 mm and 0.5 mm	
Reconstruction kernel	Smooth kernel (FC13 or FC44) with hybrid IR (AIDR 3D, Canon Medical Systems) for ViSION and ultra-high-resolution CT Full IR (FIRST, Canon Medical Systems) for GENESIS	

BMI = body mass index, ROI = region of interest, and IR = iterative reconstruction.

Supplementary material

Table S3. Univariable and multivariable binary logistic generalized estimating equations for CCTA and FFR_{CT} measures to identify ischemia.

	Univariable			Multivariable		
	X^2	OR (95% CI)	*P* value	X^2	OR (95% CI)	*P* value
CCTA†	6.8	8.0 (1.7–38.4)	**<0.01***	1.1	2.9 (0.4–21.8)	=0.30
ΔFFR_{CT}‡	21.2	18.0 (5.3–61.2)	**<0.01***	12.3	10.2 (2.8–37.3)	**<0.01***
Lesion-specific FFR_{CT}§	10.6	6.0 (2.0–17.8)	**<0.01***	2.9	3.1 (0.8–11.1)	=0.091
The lowest FFR_{CT}§	7.7	5.9 (1.8–20.4)	**<0.01***	0.01	0.9 (0.2–5.1)	=0.95

*shows statistically significance

†For CCTA, significant obstruction was defined as diameter stenosis of ≥50%.

‡For ΔFFR_{CT}, threshold value of 0.12 corresponding to the maximum Youden index was applied.

§For lesion-specific FFR_{CT} or the lowest FFR_{CT}, functional significance was defined as FFR_{CT} value of ≤0.80.

CCTA = coronary computed tomography angiography, FFR_{CT} = fractional flow reserve derived from computed tomography, OR = odds ratio, and CI = confidence interval.

Title page

Title of the manuscript

Optimized Interpretation of Fractional Flow Reserve Derived from Computed Tomography: Comparison of Three Interpretation Methods

Short title

Interpretation methods for FFR_{CT} results

Manuscript type

Original research

Authors

1. Hidenobu Takagi, MD, PhD.[a] *corresponding author*

   E-mail: hdnb69tkg@gmail.com

2. Yu Ishikawa, MD.[b]

E-mail: y.ishi@wonder.ocn.ne.jp

3. Makoto Orii, MD.[a]

   E-mail: kori931@gmail.com

4. Hideki Ota, MD. PhD.[c]

   E-mail: h-ota@rad.med.tohoku.ac.jp

5. Niiyama Masanobu, MD.[b]

   Email: dekohokuro0516@gmail.com

6. Ryoichi Tanaka, MD.[a]

   Email: rtanaka@iwate-med.ac.jp

7. Yoshihiro Morino, MD.[b]

   Email: ymorino@smile.email.ne.jp

8. Kunihiro Yoshioka, MD.[a]

   Email: kyoshi@iwate-med.ac.jp

Author affiliation

[a]Department of Radiology, Iwate Medical University, 19-1, Uchimaru, Morioka, #0208505, Japan

[b]Division of Cardiology, Department of Internal Medicine, Iwate Medical University, 19-1, Uchimaru, Morioka, #0208505, Japan

[c]Department of Diagnostic Radiology, Tohoku University, 1-1, Seiryo, Sendai, Miyagi, #9808574, Japan

Corresponding author

Hidenobu Takagi

Department of Radiology, Iwate Medical University

19-1, Uchimaru, Morioka, Iwate, #0208505, Japan

E-mail: hdnb69tkg@gmail.com

Phone: +81-19-651-5111

FAX: +81-19-622-1091

Disclosure/conflict of interest

The 6th author (YM) is speaker bureau for Abbott Vascular. Other authors declare that they have no conflict of interests.

Table of Content Summary

A standardized system for interpreting FFR_{CT} values for ischemia detection is necessary in clinical settings. Adding ΔFFR_{CT}, lesion-specific FFR_{CT}, and the lowest FFR_{CT} to the diameter stenosis showed improvements in discriminating and effectively reclassifying ischemia, with ΔFFR_{CT} being superior among the three measurements in ischemia detection. In contrast, the lowest FFR_{CT} was of limited value, suggesting that positional difference between FFR_{CT} and invasive FFR may have a potential harm; thus, FFR_{CT} values should be interpreted clinically with caution.